



## Article

# Flange Contribution to the Shear Strength of RC T-Beams with Flange in Compression

Osman M. Ramadan <sup>1,2</sup> , Ahmed H. Abdel-Kareem <sup>3</sup>, Ibrahim A. El-Azab <sup>3,\*</sup>  and Hala R. Abousafa <sup>3</sup>

<sup>1</sup> Department of Structural Engineering, Cairo University, Cairo 12613, Egypt; omoramadan@yahoo.ca

<sup>2</sup> Higher Technological Institute, HTI, 10th of Ramadan City 44629, Egypt

<sup>3</sup> Department of Civil Engineering, Benha University, Benha 13518, Egypt; ahmed.abdelkareem@bhit.bu.edu.eg (A.H.A.-K.); hala.abusafa@bhit.bu.edu.eg (H.R.A.)

\* Correspondence: ibrahim.elazab@bhit.bu.edu.eg; Tel.: +20-112-0777565

**Abstract:** As is well known, in the current design codes, the shear strength of beams is calculated based on the modified truss theory, which does not consider the effects of the flange area of T-beams. The main objective of this paper was to gain a better understanding and enhance the experimental database of the shear behavior of RC T-beams and illustrate the contribution of the flange to the shear capacity of T-beams. To accomplish this aim, a specially designed experimental program was executed, and its test results were analyzed. The main investigated variables were flange dimensions (thickness and width) and its reinforcement (longitudinal and/or vertical). Nineteen simply supported beam specimens were tested to failure under a load configuration made of two concentrated loads. Eighteen specimens had T-shaped cross-sections, while one specimen had a rectangular cross-section for comparison purposes. The items monitored during testing included the development of diagonal cracks, concrete strains, reinforcement strains, maximum loads, and deflections. Test results showed a notable increase in the shear strength of T-beams compared to rectangular beams with the same web size. For the range of variables investigated, increasing the flange thickness-to-beam depth ratio ( $\rho_t$ ) from 0.3 to 0.5 increased the shear capacity by up to 54%. In addition, increasing the flange width-to-web width ratio ( $\rho_b$ ) from 3 to 5 increased the shear capacity by up to 19%. It was also shown that the results of three-dimensional finite element (FE) analyses using ANSYS compared reasonably well with the test results for all specimens. Finally, based on the test and FE results, a simplified method that accounts for the contribution of the flange to shear capacity was proposed.

**Keywords:** reinforced concrete; flanged sections; shear strength; diagonal cracks; concrete girders; bridges



**Citation:** Ramadan, O.M.; Abdel-Kareem, A.H.; El-Azab, I.A.; Abousafa, H.R. Flange Contribution to the Shear Strength of RC T-Beams with Flange in Compression. *Buildings* **2022**, *12*, 803. <https://doi.org/10.3390/buildings12060803>

Academic Editors: Maria Polese and Marco Gaetani d'Aragona

Received: 8 May 2022

Accepted: 8 June 2022

Published: 10 June 2022

**Publisher's Note:** MDPI stays neutral with regard to jurisdictional claims in published maps and institutional affiliations.



**Copyright:** © 2022 by the authors. Licensee MDPI, Basel, Switzerland. This article is an open access article distributed under the terms and conditions of the Creative Commons Attribution (CC BY) license (<https://creativecommons.org/licenses/by/4.0/>).

## 1. Introduction

Flanged RC beams are widely utilized in the construction of civil engineering structures such as bridge decks as well as floors of residential, commercial, industrial, and other buildings. A notable application of RC thick-flanged T-beams is the main girders supporting precast beams and slabs of bridges and multi-story parking buildings. Current practice evaluates the shear resistance of RC T-beams utilizing the area of the beam web only. However, this study provides experimental and theoretical results that prove the significant contribution of flanges to the beam shear strength. The focus is on beams with the flanges subject to compressive stresses due to the bending moment. Experimental as well as finite element results show that compressed thick flanges participate significantly in the shear resistance of flanged sections. Therefore, the contribution of the flange in the T-beam should not be neglected in such cases.

An obvious contribution of the flanges to the shear capacity was illustrated in many previous studies. For example, Alberto et al. [1] showed that the contribution of flanges may lead to significant cost savings in new structures and might be decisive in assessing

the shear capacity of existing structures. An analytical model was used to analyze the shear response of beams with different geometry and main longitudinal reinforcement in the web. It has been found that, to a certain extent, the contribution of flanges to the shear capacity increased as the amount of web longitudinal reinforcement decreased. Increasing the width and thickness of the flange led to the increase in the contribution of the flanges to the shear capacity. Moreover, the maximum contribution of flanges found in the study was 31.3% of the total shear resisted. Furthermore, Amna et al. [2] studied the shear behavior of lightweight-reinforced concrete T-beams by the experimental and FE model. This study showed that T-beams with different flange widths decreased vertical deflection, longitudinal steel strain, stirrup steel strain, and the compressive concrete strain. In the event of failure, the shear stresses tended to concentrate in the flexure around the neutral axis in the compressed concrete area. In addition, Sarsam et al. [3] studied T-beams failing in shear available from the literature to estimate the influence of flanges on the shear capacity of RC beams, where an equation for predicting the contribution of the flange to shear capacity in T-beams was presented.

The effect of the shear span-to-depth ratio ( $a/d$ ) in T-beams was investigated in previous studies, e.g., [4–7]. Wakjira and Ebead [4] observed an increase in retrofit effectiveness for higher  $a/d$  ratios on the effectiveness of shear retrofitting schemes for SRG-strengthened beams. Tetta et al. made similar observations. The authors of [5] observed a doubling in strengthening effectiveness for increasing  $a/d$  ratios (1.6 to 2.6) for TRM-strengthened beams, whereas the effect of reduced shear capacity with increased shear span is generally observed in the literature [6], which can be explained by the formation of a concrete arch, i.e., a more pronounced share of the shear resistance being transferred via a diagonal compression strut for beams with a smaller  $a/d$ . Samad et al. studied the shear behavior of a reinforced concrete consisting of two reinforced concrete T-beams having similar variables and parameters with a longitudinal reinforcement of  $\rho = 2.15\%$  and a shear span-to-effective depth ratio ( $a/d$ ) of 3.5. Shear reinforcement or stirrups were added to the specimen and its spacing of stirrups was provided with the provisions of the codes where the findings of this study indicated that ACI318-08 and EC2 design codes showed significant differences in determining its shear strength capacity  $V_n$  and concrete shear resistance  $V_c$  of the T-beams [7].

The shear strength of RC T-beams without stirrups was studied in [8–10]. Thamrin et al. [8] found that the shear strength of T-beams was affected by both the flange size and the main longitudinal reinforcement in the web. According to test data, T-beams had a shear capacity of 5% to 20% higher than those of rectangular beams with the same web dimensions. Moreover, according to the researchers, the angle of the diagonal crack was also influenced by the web longitudinal reinforcement ratio in the shear span. Furthermore, the shear strength of slender-reinforced concrete beams with and without shear reinforcement was studied using a mechanical model [9]. For beams with T- or I-sections, for instance, the contribution of the concrete compression chord may be very important, as opposed to what is considered by most existing codes. Reinforced concrete T beams without stirrups in experimental research [10] were tested in the laboratory for shear strength, and the results indicated enhanced shear strength for beams with a flange.

The use of fiber-reinforced polymer sheets is a well-studied area of research for RC T-beams and, in particular, many experimental campaigns have been carried out for monotonic loading, e.g., [11,12]. Etman [13] showed that strengthening RC T-beams in the shear zone using carbon-fiber-reinforced polymer (CFRP) enhanced the shear capacity of existing RC beams, which showed that the use of the CFRP sheet reflected higher specimen stiffness, compared to steel. Another experimental study [14] was designed to assess the effects of increased steel shear reinforcement, changes in shear span-to-depth ratios, as well as the effect of different retrofit layouts and materials (the use of fiber-reinforced polymer and textile-reinforced mortars), where the experimental results were used to calibrate a detailed nonlinear finite element analysis to further complete the parametric study, and it was found that the parameters of interest do influence the retrofit effectiveness.

Over the years, a great amount of experimental and theoretical research has been conducted, resulting in significant advancements in our understanding of the shear resisting process. Consequently, empirical and rational models capable of predicting the experimental performance have been developed, including assessment codes [15–17]. Nevertheless, the majority of these models were developed exclusively for elements with rectangular cross-sections.

An experimental study [18] showed that slender-reinforced concrete (RC) beams with a thin T-shaped section have a higher shear strength than beams without flanges that have the same depth, web width, and reinforcement amounts. For instance, reference [19] demonstrated that the shear strength of T-beams is often 30% to 40% larger than the shear strength of the beam web alone. Furthermore, several theoretical models, e.g., [20–25], acknowledged the good contribution of the flanges to shear strength. Despite this mass of published research, it does not adequately cover flanged beams with thick, wide flanges.

In our study, a test setup and program were developed to investigate the performance of T-beams with thick and wide flanges in compression. The study variables were flange dimensions and flange reinforcement. Nineteen simply supported specimens were tested until failure under the effect of two concentrated loads acting at the third points of the beam span. Eighteen specimens had T-shaped cross-sections, while the remaining one had a rectangular cross-section for comparison purposes. In addition, thirty-four 3D nonlinear finite element models were analyzed using ANSYS to complement the data needed to develop a simplified method that accounts for the flange contribution to beam shear strength. The objective was to determine the thick flange contribution to shear strength when exposed to compressive stresses and to try to find a suitable analytical model.

## 2. Research Significance

The flange thickness-to-web depth ratio in most bridges and buildings is larger than cast in situ buildings. “The flange’s thickness may reach half the depth of the web”. Thus, it appears unwise to abstract the flange’s contribution in shear strength as is actually performed by the diverse designed codes [15–17]. That is, ACI 318-19 and ECP-203 do not employ any contribution of the flange in shear resistance. Therefore, this paper applies experimental and theoretical studies that achieve considerable benefits in the field of the construction industry, when the shear strength of the “flange in the compression” is calculated and takes an important term in the shear equation based on the proofs of our experimental and theoretical studies. We use test specimens without stirrups in the web to avoid exceeding the shear capacity of the test frame. It is shown that using such specimens does not affect the evaluation of the flange contribution to shear strength through the analysis of FE results for all test specimens considering the two situations of with and without web stirrups.

## 3. Experimental Work

### 3.1. Test Program

The experimental program includes 19 specimens, eighteen of which are simply supported beams and one of which is a control specimen with a rectangular section. The T-section specimens are divided into 6 groups where each group contains 3 specimens. The specimens in various groups differ with respect to flange thickness-to-web depth ratio ( $\rho_t = t_f/h$ ), flange width ratio ( $\rho_b = b_f/b_w$ ), and flange longitudinal reinforcement. The tested specimen length is 1400 mm with a depth of 300 mm, web width of 100 mm, and overall span of 1300 mm. This gives a span-to-depth ratio ( $l/h$ ) of larger than 4. To avoid bearing failure, the web is widened (as wide as the flange) at support zones. In addition, the beam is reinforced with two vertical U-shaped bars  $\varnothing 10$  and three horizontal stirrups  $\varnothing 6$  at support zones.

No shear reinforcement within the shear zone “transverse reinforcement” is used in the beam web, as shown in Figure 1, as the shear strength contribution of the flange is focused on, which minimizes the required test load as well. Consequently, the relative

increase in shear strength due to the flange existence is large compared to those of similar beams without a flange.

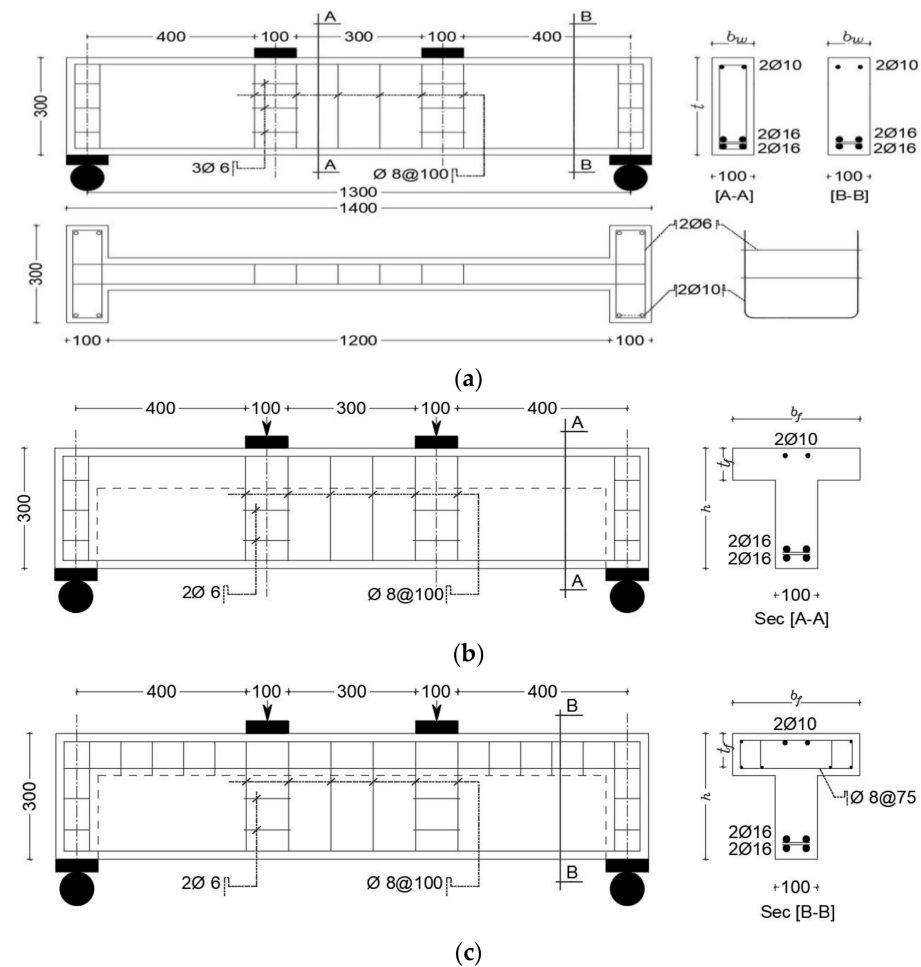


**Figure 1.** Specimen details and arrangement of reinforcement (all dimensions are in mm). (a) Specimen with rectangular cross-section (control); (b) specimen with T-cross-section without stirrups in flange; (c) specimen with T-cross-section with stirrups within flange.

The specimens are loaded until the failure occurs with two-point loads that gives a shear span-to-depth ratio equal to 1.5. A 1000 kN capacity hydraulic jack is used in loading. All specimens are designed to motivate shear failure before flexural failure occurs. Figure 1 presents the typical details of the tested specimens. The main bottom reinforcement is about four steel bars in all specimens  $\varnothing 16$  (diameter of 16 mm and area of 201 mm<sup>2</sup>), which are laid in two layers at the bottom of the beam cross-section and two  $\varnothing 10$  bars (diameter of 10 mm and area of 78.54 mm<sup>2</sup>) laid in one layer at the top. To avoid causing early anchorage failure, the bottom and top bars are anchored at the support with 90-degree hooks. The web reinforcement has a  $\varnothing 8@100$  mm spacing in the middle part between two applied loads. For flanged beams with longitudinal reinforcement, the ratio of longitudinal reinforcement in the flange is nearly 1%; for the flange concrete area, the stirrups have a  $\varnothing 8@75$  mm spacing; and the branches have a spacing of 100 mm, as shown in Figure 2. Notice that all beams are not provided with shear reinforcement in the web at the shear critical zone, to keep the failure loads at small values. This happens as the main goal of the tests is to quantify the increase in shear strength due to flange existence.



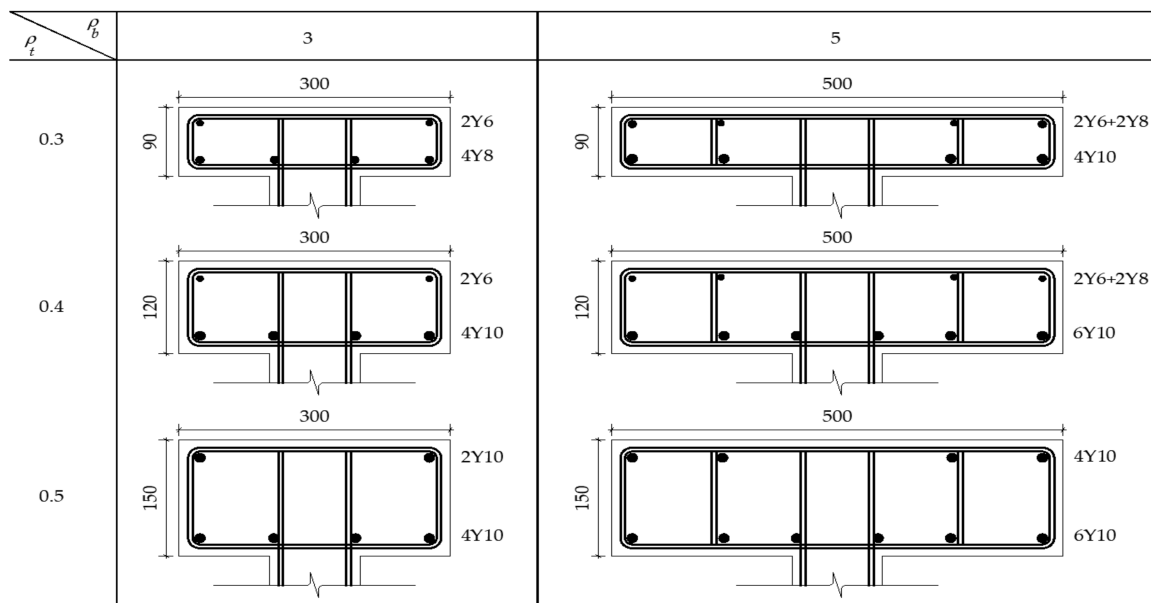


**Figure 2.** Arrangement of longitudinal reinforcement and “stirrups out of shear zone” in the flange.

In Table 1, each specimen is given a code consisting of three parts: the first part refers to reinforcement in the flange (G1 without reinforcement, G2 with longitudinal reinforcement, and G3 with longitudinal and flange stirrups within the two shear zones); the second part refers to the ratio of flange thickness “flange thickness to depth” ( $\rho_t = 0.3, 0.4$ , and  $0.5$ ); and the third part refers to the flange width “width ratio” ( $\rho_b = 3$  for flange width equal to 300 mm and 5 for flange width equal to 500 mm).

**Table 1.** Experimental Program.

Specimen	$f_{cur}$ (Mpa)	Cross- Sectional Area (cm <sup>2</sup> )	Cross-Sec. Area Increasing (%)	Flange Dim.		Stirrups in Flange	Longitudinal Reinforcement in Flange		Longitudinal Reinforcement %
				$\rho_t$	$\rho_b$		Bottom	Top	
C0	36.4	300	—	—	3	—	—	—	
G1-0.3-3	36.4	480	60%	90/h = 0.3		—	—	—	
G2-0.4-3	36.4					—	4 Ø 8	3 Ø 6	1.055%
G3-0.5-3	36.4					Ø8@75	—	—	
G1-0.3-3	34.2	540	80%	120/h = 0.4		—	—	—	
G2-0.4-3	34.2					—	4 Ø 10	2 Ø 6	1.029%
G3-0.5-3	34.2					Ø8@75	—	—	
G1-0.3-3	34.2	600	100%	150/h = 0.5		—	—	—	
G2-0.4-3	36.8					—	4 Ø 10	2 Ø 10	1.047%
G3-0.5-3	36.8				Ø8@75	—	—		
G1-0.3-5	36.8	660	120%	90/h = 0.3	5	—	—	—	
G2-0.4-5	35.6					—	4 Ø 10	2 Ø 6 + 2 Ø 8	1.046%
G3-0.5-5	35.6					Ø8@75	—	—	
G1-0.3-5	35.6	780	160%	120/h = 0.4		—	—	—	
G2-0.4-5	35.6					—	6 Ø 10	2 Ø 8 + 2 Ø 6	1.046%
G3-0.5-5	35.6					Ø8@75	—	—	
G1-0.3-5	34.8	900	200%	150/h = 0.5		—	—	—	
G2-0.4-5	34.8					—	6 Ø 10	4 Ø 10	1.046%
G3-0.5-5	34.8					Ø8@75	—	—	

### 3.2. Material Properties

Table 1 summarizes the average values of compressive strength of the concrete cube strength ( $f_{cu}$ ). The results are calculated from the average values of three samples. The concrete mixture of test specimens casting contains ordinary Portland cement, irregular gravel of a maximum size of 15 mm, and sand with a finesse modulus equal to 0.5 mm. The water–cement ratio is 0.45. Both high- and normal-steel-strength bars are tested in tension for high-tensile steel  $f_y = 420$  MPa and normal  $f_y = 240$  MPa.

### 3.3. Test Setup and Instrumentation

The experimental study applies the test setup of rigid steel frames, which are supported by a rigid floor in the reinforced concrete laboratory. A hydraulic jack of 1000 kN capacity is utilized for equally distributed loading of two concentrated points symmetrically 400 mm apart at an overall span of 1300 mm, as in Figure 3. The loading is recorded by the load cell connected to a data logger. To monitor the deflection, three Linear Variable Differential Transformers (LVDTs) are placed under the center and the two load points of the beam. The strain gauges are utilized to gauge the strain in the longitudinal reinforcement in the flange at the shear zone.

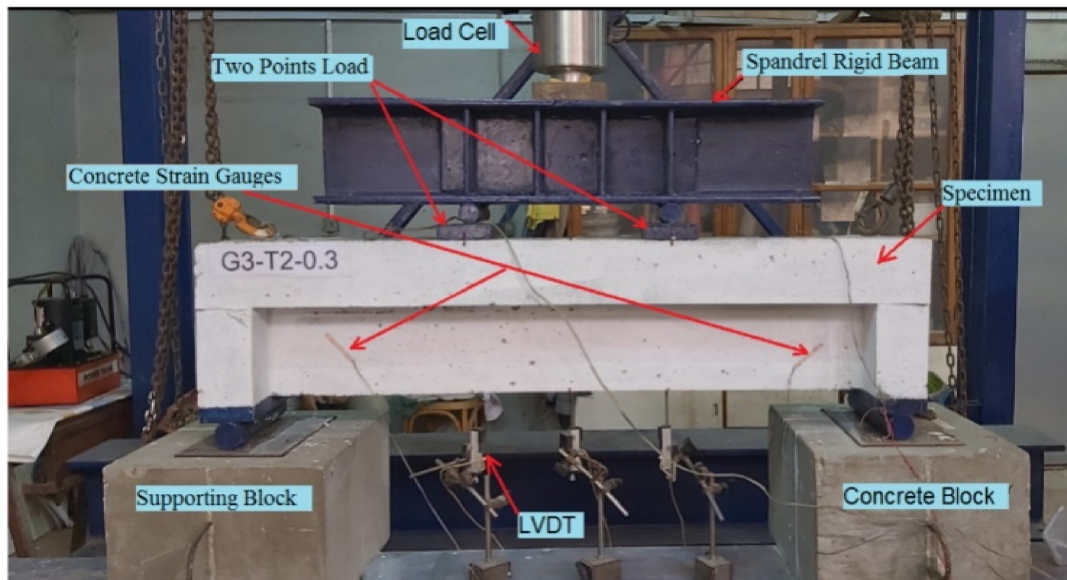


Figure 3. Test setup.

## 4. Results

For both rectangular and flanged beams, when the concrete reached its tensile strength, cracks developed in the high shear region, leading to collapse. In the following, the test results are discussed in terms of:

1. The load at collapse and the profit in capacity due to the flange dimensions and reinforcement.
2. The load versus deflection relationship.
3. The cracking pattern and failure modes.
4. The strains in the concrete and in flange longitudinal steel.

Table 2 presents the maximum load for specimens with T-sections higher than the rectangular section based on the flange thickness, longitudinal reinforcement in the flange, and due to subjecting the flange to compressive stresses. This actuality confirms that the flange in T-beams has a positive effect on the shear stress distribution and diffusion of the diagonal cracks in the web.

**Table 2.** Experimental results of specimens.

Specimen	$f_{cu}$ (Mpa)	$\rho_t$	$\rho_b$	$\zeta$	Cracking Load $P_{cr}$ (kN)	Ultimate Load $P_u$ (kN)	$\frac{P_u - P_{u,c}}{P_{u,c}}$ %	Max. Recorded Deflection (mm)	Mode of Failure
C0	36.4	—	—	—	95	106	0	2.33	
G1-0.3-3	36.4	0.3	—	—	100	282	165	4.74	
G1-0.4-3	36.4	0.4	—	—	105	363	241	5.97	
G1-0.5-3	36.4	0.5	—	—	110	431	305	5.98	
G2-0.3-3	34.2	0.3	1.055	—	90	326	207	5.80	Shear
G2-0.4-3	34.2	0.4	3	1.029	105	377	255	5.87	
G2-0.5-3	34.2	0.5	1.047	—	115	439	312	4.43	
G3-0.3-3	34.2	0.3	1.055	—	110	358	237	5.89	
G3-0.4-3	36.8	0.4	1.029	—	100	384	261	7.07	
G3-0.5-3	36.8	0.5	1.047	—	115	454	327	6.22	
G1-0.3-5	36.8	0.3	—	—	115	299	181	4.49	
G1-0.4-5	35.6	0.4	—	—	120	392	268	4.79	
G1-0.5-5	35.6	0.5	—	—	115	432	307	6.59	
G2-0.3-5	35.6	0.3	1.046	—	110	342	221	5.11	
G2-0.4-5	35.6	0.4	5	1.046	120	383	260	6.51	Shear
G2-0.5-5	35.6	0.5	1.046	—	115	446	320	9.11	
G3-0.3-5	34.8	0.3	1.046	—	95	429	304	8.05	
G3-0.4-5	34.8	0.4	1.046	—	85	437	311	9.56	
G3-0.5-5	34.8	0.5	1.046	—	125	474	346	10.13	

$\zeta$ : Longitudinal reinforcement ratio in flange,  $\rho_t$ : depth ratio ( $t_f/h$ ),  $\rho_b$ : width ratio ( $b_f/b_w$ ),  $P_{u,c}$ : ultimate load of control specimen.

#### 4.1. The Effect of Web Reinforcement

One factor that affects the design of test specimens is the capacity of the test frame. In this study, the tests were conducted at the reinforced concrete laboratory of the Faculty of Engineering, Benha University, which has a test frame with a capacity of approximately 60 t. As our initial calculations of the specimen capacity were close to this maximum value, a few options were considered to reduce the maximum required load. As the study focused on the flange contribution to shear strength, one choice was to use specimens without stirrups in the web (within the test shear zone). This way, the maximum shear capacity of specimens was reduced to below 60 t. To verify that the use of such specimens will not affect the experimental evaluation of flange contribution to shear strength, we first analyzed FE models of all test specimens for the two cases of with and without web stirrups. An evaluation of the error in the FE estimates of the flange's contribution to shear resistance in the absence of web stirrups is provided in Section 6 below.

#### 4.2. Ultimate Load

Figure 4 shows a comparison of ultimate load ( $P_u$ ) among all tested specimens. It is obvious that an increase in the dimensions of the flange, either the width or the depth, generally gave an increase in  $P_u$ . By increasing the width ratio  $\rho_b$  from 3 to 5, the ultimate load  $P_u$  increased from 6% to 8% for the first group, which did not have any reinforcement in the flange. This is in line with results published in [10] where increasing the effective flange width ratio from 1 to 6 increased the shear strength by about 10 to 30%. When compared to the rectangular specimen “control”, we found that  $P_u$  increased by 165% to 307% due to the existence of compressed thick flanges, a result that agrees with a previous remark that the contribution of concrete compression for beams with T-section chords may be very important, as opposed to what is considered by most existing codes [9].

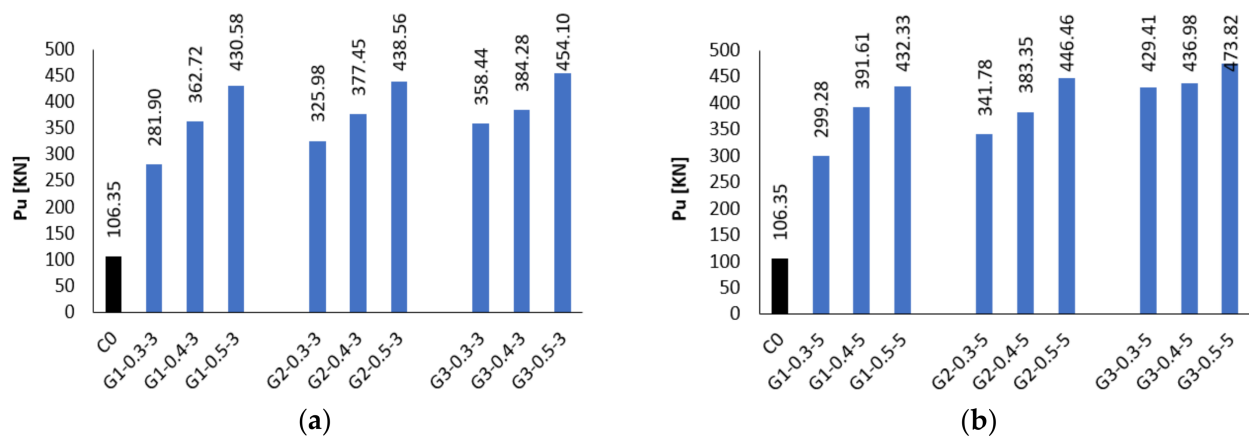


**Figure 4.** Max. ultimate load ( $P_u$ ) for all specimens. (a) Specimens (control & width ratio  $p_b = 3$ ), (b) Specimens (control & width ratio  $p_b = 5$ ).

The increasing depth ratio  $\rho_t$  led to an enhancement in the ultimate load for flanged specimens. As for increasing  $\rho_t$  from 0.3 to 0.5, it led to increasing  $P_u$  from 29% to 53% of specimens having  $\rho_b = 3$ , and from 31% to 44% for specimens having  $\rho_b = 5$ . This compares well with Alberto et al. [1] who noted that increasing the width and thickness of the flange increased the contribution of the flanges to shear capacity. Specifically, they found that the maximum contribution of flanges was 31.3% of the total shear resisted. In addition, Thamrin et al. [8] used test data to show that the shear strength of T-beams was 5% to 20% higher than rectangular beams with the same web dimensions. In this study, the existence of the longitudinal reinforcement to the flange induced the increase in the ultimate load in the range from 207% to 320% when compared with the control specimen, whereas, during the comparison with the first group, we found an enhancement in  $P_u$  from 2% to 16%. In addition, the existence of stirrups with longitudinal reinforcement in the flange induced an increase in the ultimate load in the range from 5% to 43% when compared with the first group without any reinforcement in the flange.

#### 4.3. Load–Deflection Relationship

It is very clear from Figure 5 that the load–deflection relationship of the RC T-beam was quite different from that of the corresponding rectangular beam. Furthermore, the shear strength of the flanged beam was higher than that of the corresponding rectangular specimen. After the first diagonal crack appeared, a larger deflection was observed with increasing load, especially for specimens without longitudinal reinforcement in the flange. Specimens with different flange dimensions and reinforcement were tested and their results were compared to those of the rectangular beam “control specimen”. At 25%  $P_u$  of the control specimen, the deflection of specimens with the longitudinal reinforcement decreased by 30–80% with respect to the deflection of the control specimen.

There was a very good control on mid-span deflection when the longitudinal reinforcement was added in the flange, where a large reduction in the deflection in the same load existed, as is well known from other experiments and FE analyses [2].

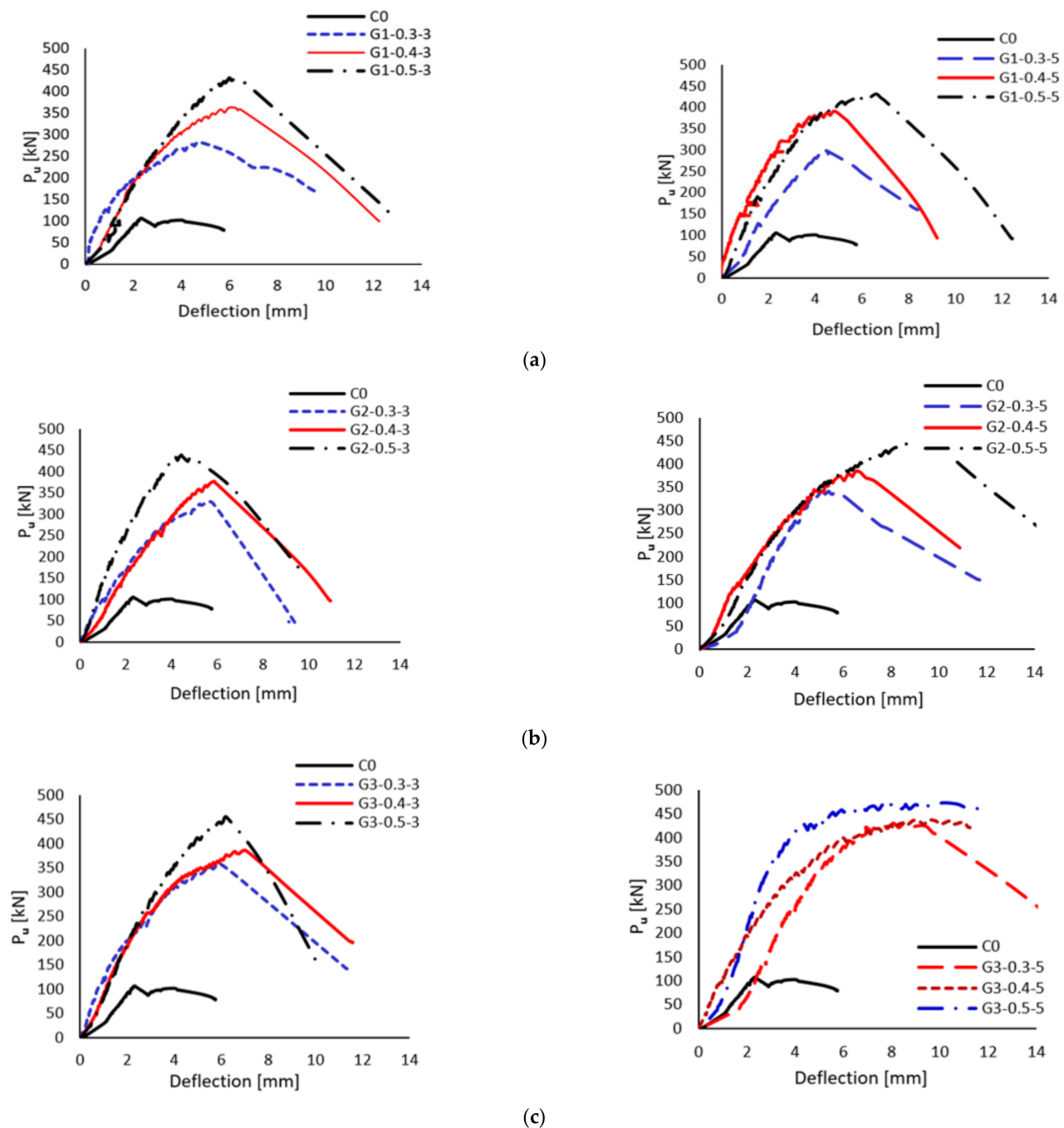


**Figure 5.** Load–deflection relationship for control specimen and other specimens with various flange thicknesses at flange width ratios of 3 and 5. (a) Specimens without reinforcement in flange. (b) Specimens with longitudinal reinforcement in flange. (c) Specimens with longitudinal steel and stirrups in flange.

The load–deflection curves of the tested specimens are shown in Figure 5. There is an important observation of beam capacity that increased as the depth ratio ( $\rho_t$ ) and width ratio ( $\rho_b$ ) of the flange increased, in addition to the shear capacity “strength” afflicted with the existence of longitudinal reinforcement within the flange. By contrast, after longitudinal reinforcement, the specimens G3-0.4-5 and G3-0.5-5 failed in shear (Figure 5). This is obvious in the load–deflection curve of the straight line in the end part “improvement the ductility”. Moreover, the reinforcement in specimens G3-0.3-3 and G3-0.3-5 did not reach the yield strength until the occurrence of shear failure. Load–deflection curves of



rectangular and flange beams are compared in Figure 5. The contribution of the flange in the compression zone led to an increase in the capacity and stiffness of beams with T-sections compared to those of beams with rectangular sections and to an improvement in the shear strength.

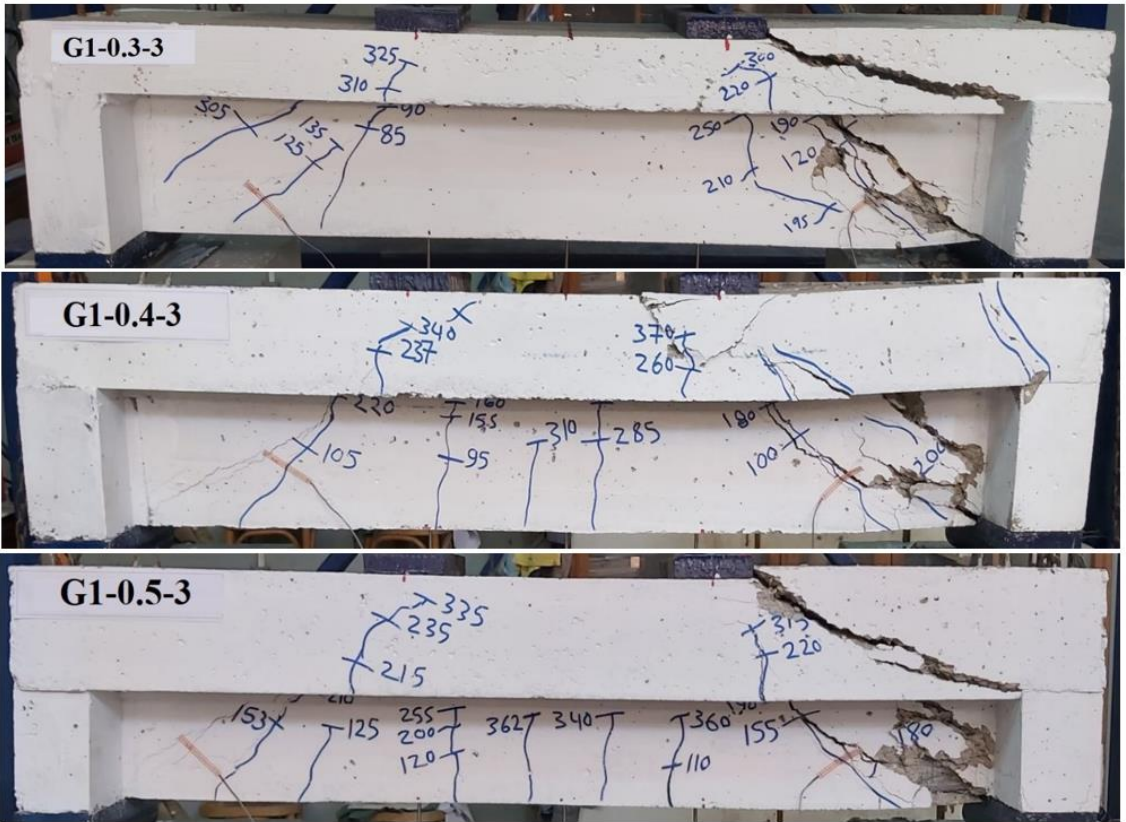
#### 4.4. Cracking Pattern and Modes of Failure

During the initial part of the test, as the applied load was increased, hair “shear” cracks started to appear near the supports, as shown in Figure 6b–g. With the further increase in the load, more shear cracks were initiated near the supports. Then, cracks propagated within the beam web in inclined paths at angles from  $45^\circ$  to  $65^\circ$  with the longitudinal axis of the beam. Subsequently, the cracks extended into the beam flange (Figure 6b–g), but with a smaller cracking angle. Finally, one or more cracks continued to propagate and widen within the beam full depth until failure took place. The cracking load of the rectangular (control) specimen was about 89% of the maximum load (recall that no web reinforcement was provided). Nevertheless, the diagonal cracks in flanged specimens appeared at a load of about 19% to 30% of the maximum load (recall that web reinforcement was provided in flange only). Failure modes for all specimens are described in Table 2. Crack patterns and the propagation process varied depending on flange thickness, width, and reinforcement. The inclination of the shear crack with the beam longitudinal axis was much smaller ( $\approx 15^\circ$  to  $25^\circ$ ) than it was within the beam web ( $45^\circ$  to  $65^\circ$ ). In addition, visual inspection of control specimen C0 (Figure 6a) at failure revealed that it had a wider main inclined crack compared with the corresponding cracks in flanged specimens. Finally, the presence of stirrups and longitudinal reinforcement in the flange resulted in good control of the cracks within the flange (see, for example, Figure 6g). The contribution to the shear capacity of shear transfer actions transferring stresses across cracked concrete was negligible due to the great width of the critical flexural-shear crack [26,27]. Although this is a very important aspect, it is out of the scope of this study and will be discussed with a much larger database in a future study.

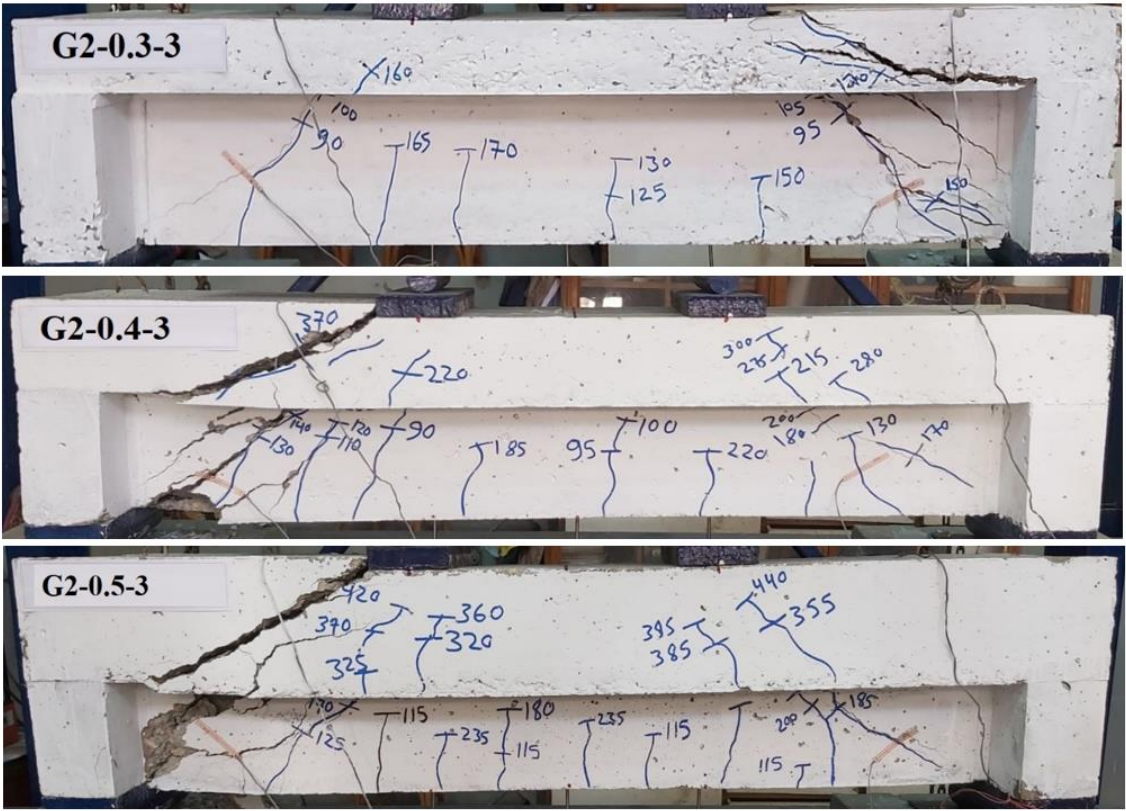


(a)

Figure 6. Cont.



(b)



(c)

Figure 6. Cont.



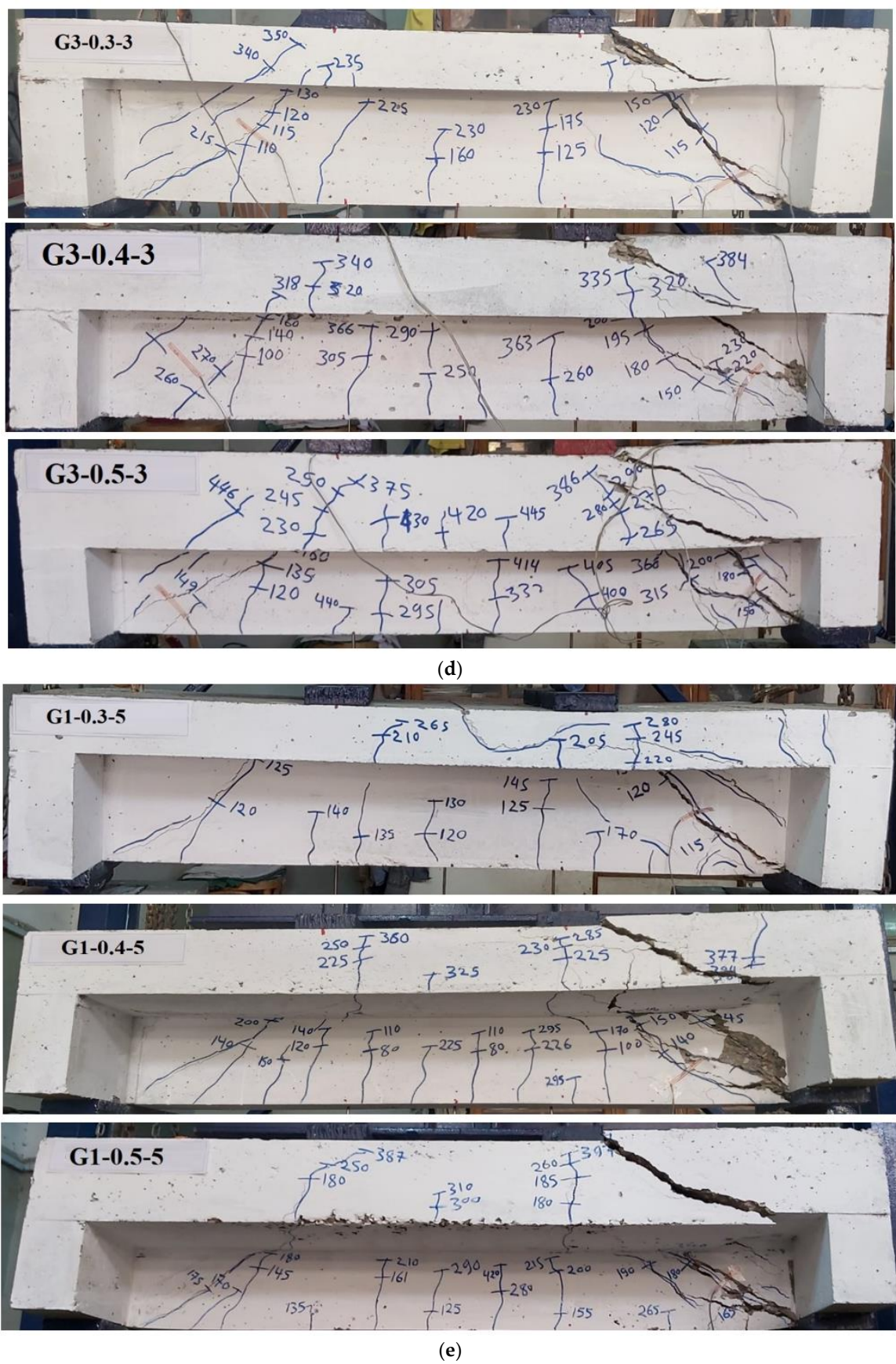
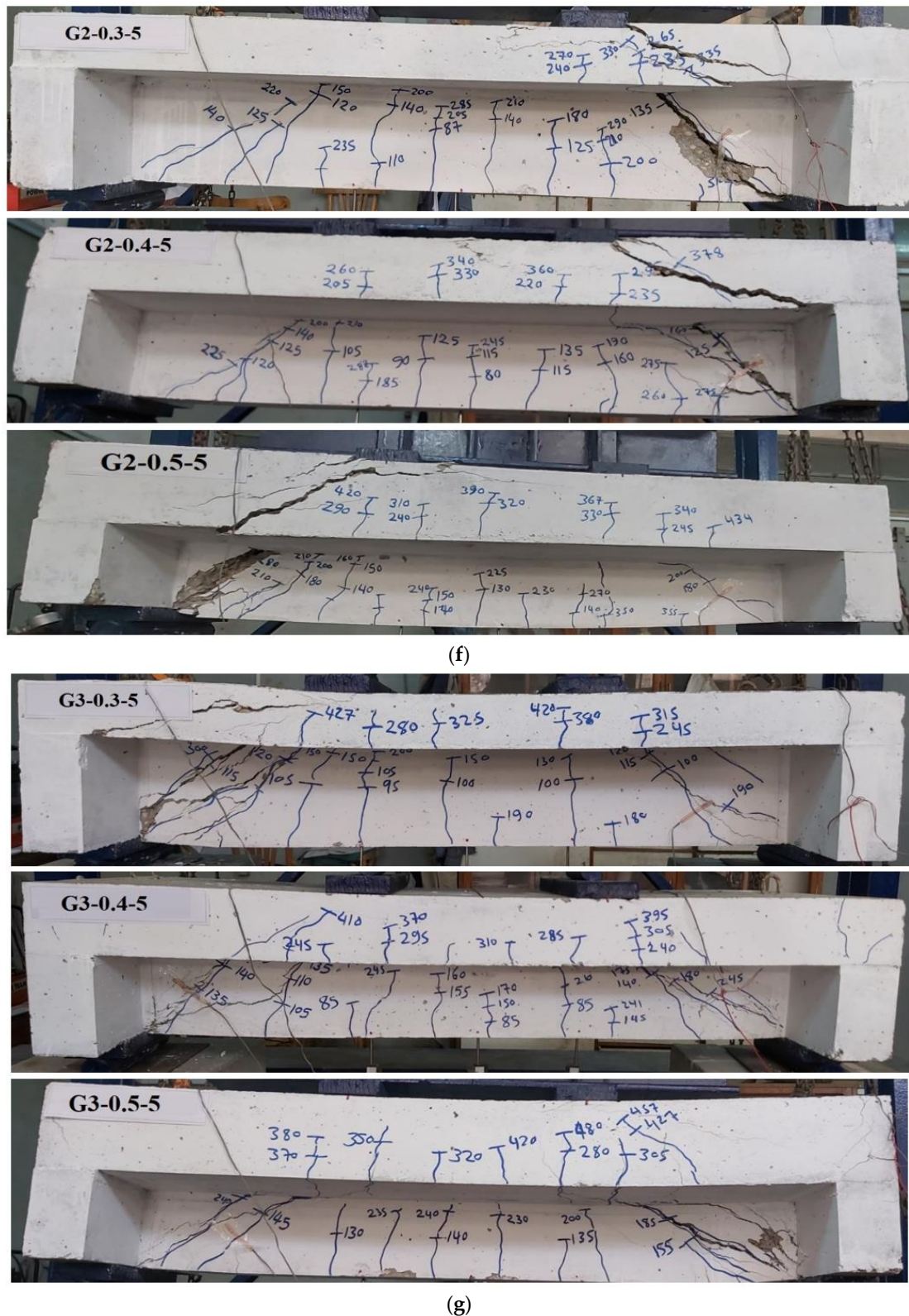


Figure 6. Cont.



**Figure 6.** Experimental crack pattern for control beam and other flanged specimens. (a) Control beam; (b) specimens without reinforcement in flange  $\rho_b = 3$ ; (c) specimens with longitudinal reinforcement in flange  $\rho_b = 3$ ; (d) specimens with longitudinal steel and stirrups in flange  $\rho_b = 3$ ; (e) specimens without reinforcement in flange  $\rho_b = 5$ ; (f) specimens with longitudinal reinforcement in flange  $\rho_b = 5$ ; (g) specimens with longitudinal steel and stirrups in flange  $\rho_b = 5$ .



#### 4.5. Strain Analysis

This part of the study investigates the strains in flange longitudinal steel and concrete. Extensive instrumentation for strain monitoring was carefully provided to collect the information needed to study the shear resistance mechanisms of flanged-reinforced concrete beams.

##### 4.5.1. Strain in Longitudinal Reinforcement in Flange

Figure 7a,b present a variation in the strains in the flange longitudinal steel with the applied shear force—for different flange thicknesses—at flange width ratios of 3 and 5, respectively. No noticeable contribution of flange steel to the shear resistance was observed prior to the initiation of the first diagonal crack. Strains started to develop in the flange longitudinal steel at an average applied load of about 95 and 125 kN “ $\approx 26$  and 29% of ultimate strength” for G2 and G3 specimens, respectively. The longitudinal steel strain continued to increase with the load until failure. For the same applied load, the strain in flange longitudinal steel was greater in the wider flange specimens with  $\rho_t = 0.5$ . It must be noted, however, that the yielding of longitudinal steel did not materialize in most cases.

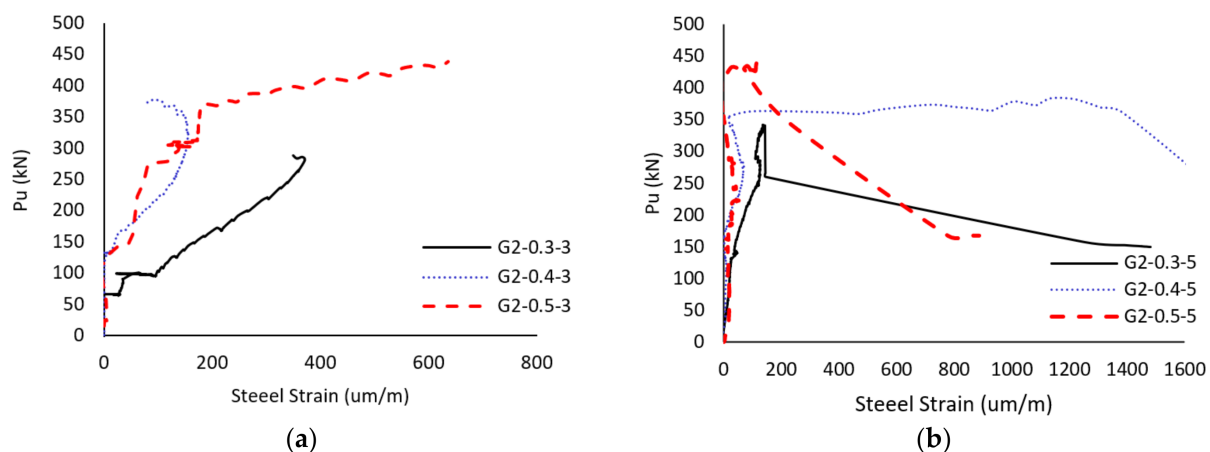


**Figure 7.** Relation between ultimate load and strains in the flange longitudinal steel for different flange thicknesses at flange width ratios of 3 and 5. (a) Specimens with  $\rho_b = 3$ ; (b) specimens with  $\rho_b = 5$ .

##### 4.5.2. Concrete Tensile Strain in Web

Figure 8a,b presents the relationship of applied force versus strains measured on the concrete web. These curves, which feature similar forms, refer to the initial phase of loading, where the compression concrete flange is practically not strained. This applied force was about 30 kN for specimens with  $\rho_b = 3$  and 140 kN for specimens with  $\rho_b = 5$ . In other words, the contribution flange works after the diagonal cracks have developed. From Figure 8, it is observed that the strain increased almost linearly with the loads until it reached approximately 200 micro-strains on average. Beyond that point, the curves featured a somewhat plastic response. Physically, this corresponded to the propagation of cracks toward the compression zone. The strain at failure attained 1000 to 1800 micro-strains on average.



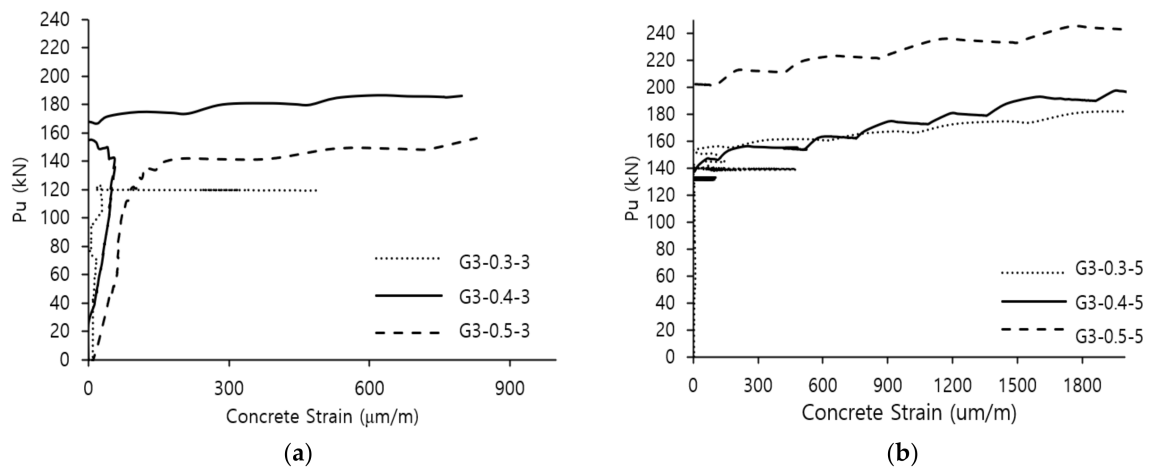


**Figure 8.** Relation between ultimate load and strains in concrete web for different flange thicknesses—at flange width ratios of 3 and 5. (a) Specimens with  $\rho_b = 3$ ; (b) specimens with  $\rho_b = 5$ .

### 5. Proposed Simplified Calculations

In international codes, such as the ACI Building Code Equation (1), and the Euro code, the shear force in a T-beam is assumed to be carried only by its web. This simplified assumption, which has prevailed in the shear design practice, is not correct for T-beams with a thick flange in the compression side. Experimental measurements as well as results of the finite element made it clear that the enhancement of shear strength due to beam flanges (when subject to compressive stresses) cannot be neglected. Analysis of all results showed that, limited to the range of parameters considered, we can conservatively assume that the total area of the flange is effective in resisting shear. Then, the shear strength of T-beams with the flange in the compression side is calculated using Figure 9 and Equations (1 and 2) as follows:

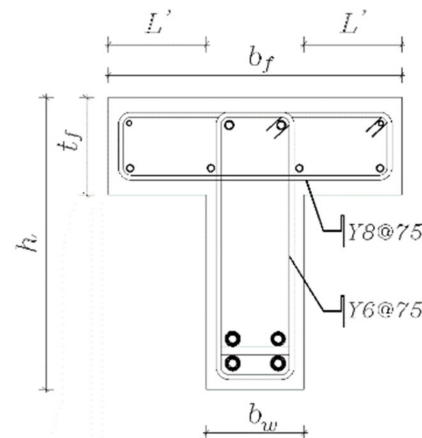


**Figure 9.** Cross-section. Range of parameters considered: width ratio ( $\rho_b = b_f/b_w \leq 5$ ), depth ratio ( $\rho_t = t_f/h$ ) up to 1,  $L' \leq 2b_w$ ; where  $L'$  is the left/right protruded part of the flange.

ACI 318M [18]—Simplified method

$$V_n = \left[ 0.17\lambda\sqrt{f'_c} \right] b_w d + \frac{A_v f_y d}{s} \quad (1)$$

where  $\lambda$  is the modification factor to reflect the reduced mechanical properties of lightweight concrete relative to normal-weight concrete of the same compressive strength, for normal-weight concrete = 1.

Proposed simplified equation for shear strength of flanged beam ( $V_{p, proposed}$ )

$$V_{p, proposed} = \left[ 0.17\lambda\sqrt{f'_c} \right] \left[ b_w d + 2L't_f \right] + \left[ \frac{A_v f_y d}{s} \right]_w + \left[ \frac{A_v f_y d}{s} \right]_f \quad (2)$$

Figure 10 depicts the 3D finite element “FE” model developed using the “ANSYS” program for the numerical analysis of all specimens with and without shear reinforcement “Groups G1 and G3”. Additional cases with different depth ratios “ $\rho_t$ ” as shown in Table 3 were also modeled to verify the accuracy of the proposed method (Equation (2)). The ANSYS program was adopted as it is successful in analyzing reinforced concrete beams, and yields results that are quite close to the experimental data [28,29]. For details of the FE modeling, please refer to [30].

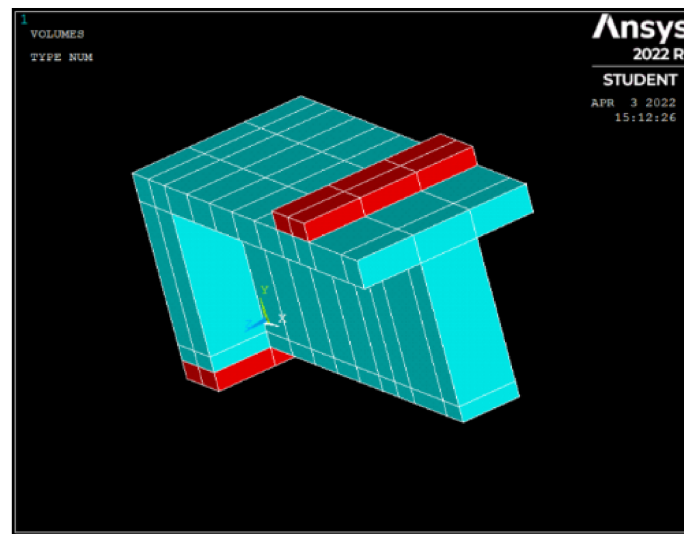


**Figure 10.** Three-dimensional model for specimens [30].

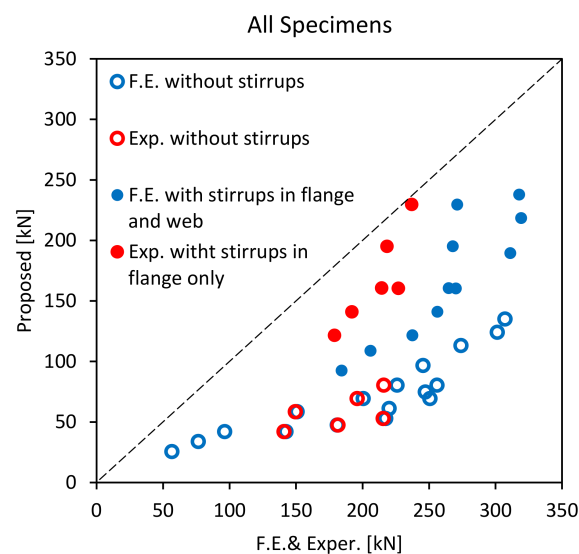
To test the adequacy of the proposed simplified method, Table 3 and Figure 11 compare results of Equation (2) with established experimental and finite element results. Both Table 3 and Figure 11 prove that Equation (2) always results in good “conservative” estimates. In particular, the results of Equation (2) for specimens with and without shear reinforcement are about (24% to 45%) and (50% to 97%) of the actual strength, while for specimens with shear reinforcement in the flange and web (G3), the ratio ranges. This is true for T-beams when the flange is subjected to compressive stresses, and the limits given above. The limits are width ratio:  $(\rho_b = b_f/b_w) \leq 5$ ; depth ratio:  $(\rho_t = t_f/h)$  of up to 1; and flange protrusion length  $L' \leq 2b_w$  on each side. Thus, Equation (2) is excessively conservative, and more research work is needed to improve these calculations.

Finally, Table 4 compares the results of the proposed method, Equation (2), and the present ACI estimates, Equation (1). This comparison illustrates that for T-beams with thick, wide flanges in compression, the actual shear strength can be as high as 486% (about five times) of the present ACI prediction. Thus, neglecting the contribution of flanges to shear strength in such cases is inappropriate.

**Table 3.** Verification of proposed equation with FE results \*.

Specimen	$f_c'$ (Mpa)	$f_{yt}$ (Mpa)	Dimensions [mm]					$A_v$ (mm <sup>2</sup> )		F.E. Method	Proposed Method (kN)					$V_P/V_{FE}$
			$b_w$	$d_w$	$L'$	$t_f$	$d_f$	$A_{v,w}$	$A_{v \cdot f}$		$V_{FE}$ (kN)	$V_c$	$V_{s-w}$	$V_{s-f}$	$V_P$	
C0	28.8	240	100	280	0	0	0	0.00	0.00	56.7	25.54	0.00	0.00	25.54	0.45	
G1-0.15-3					100	45	25			76.5	33.76			33.76	0.44	
G1-0.30-3						90	70			142.4	41.97			41.97	0.29	
G1-0.40-3						120	100			181.0	47.44			47.44	0.26	
G1-0.50-3						150	130			217.5	52.91			52.91	0.24	
G1-0.65-3						195	175			220.1	61.13			61.13	0.28	
G1-0.80-3						240	220			250.8	69.34			69.34	0.28	
G1-0.90-3						270	250			247.3	74.81			74.81	0.30	
G1-1-3						300	280			256.0	76.63			76.63	0.30	
G1-0.15-5					200	45	25			96.4	41.97			41.97	0.44	
G1-0.30-5						90	70			150.9	58.39			58.39	0.39	
G1-0.40-5						120	100			200.6	69.34			69.34	0.35	
G1-0.50-5						150	130			226.0	80.28			80.28	0.36	
G1-0.65-5						195	175			245.5	96.71			96.71	0.39	
G1-0.80-5						240	220			274.0	113.13			113.13	0.41	
G1-0.90-5						270	250			301.4	124.07			124.07	0.41	
G1-1-5						300	280			307.2	127.72			127.72	0.42	
C0-S					280	0	0			0	56.6			0	116.50	25.54
G3-0.15-3				235	100	45	25	56.6	201	184.28	33.76	42.56	16.10	92.41	0.50	
G3-0.30-3				190		90	70			237.50	41.97	34.41	45.07	121.45	0.51	
G3-0.40-3				160		120	100			256.30	47.44	28.98	64.38	140.80	0.55	
G3-0.50-3				130		150	130			270.20	52.91	23.55	83.70	160.16	0.59	
G3-0.65-3				85		195	175			311.12	61.13	15.40	112.67	189.19	0.61	
G3-0.80-3				40		240	220			319.25	69.34	7.24	141.64	218.23	0.68	
G3-0.90-3				10		270	250			317.78	74.81	1.81	160.96	237.58	0.75	
G3-1-3				0		300	280			350.56	76.63	0.00	180.28	256.91	0.73	
G3-0.15-5				235	200	45	25	56.6	302	205.95	41.97	42.56	24.14	108.67	0.53	
G3-0.30-5				190		90	70			264.80	58.39	34.41	67.60	160.40	0.61	
G3-0.40-5				160		120	100			267.80	69.34	28.98	96.58	194.89	0.73	
G3-0.50-5				130		150	130			271.20	80.28	23.55	125.55	229.38	0.85	
G3-0.65-5				85		195	175			356.74	96.71	15.40	169.01	281.11	0.79	
G3-0.80-5				40		240	220			369.52	113.13	7.24	212.47	332.84	0.90	
G3-0.90-5				10		270	250			392.70	124.07	1.81	241.44	367.33	0.94	
G3-1-5				0		300	280			411.71	127.72	0.00	270.41	398.14	0.97	

\* NOTE: Group G1 are beams without stirrups in web and flange, while Group G3 is with stirrups in web and flange.  $A_{v,w}$ : area of web stirrups;  $A_{v,f}$ : area of flange stirrups;  $V_c$ : nominal shear strength provided by concrete;  $V_{s,w}$ : nominal shear strength provided by web shear reinforcement;  $V_{s,f}$ : nominal shear strength provided by flange shear reinforcement.

**Figure 11.** Correlation between the proposal, FE, and the experimental results.

**Table 4.** Comparison of proposed equation with ACI.

Specimen	$f_c'$ (Mpa)	$f_{yt}$ (Mpa)	Dimensions [mm]					$A_v$ (mm <sup>2</sup> )		ACI	Proposed Method (kN)					$V_P/V_{ACI}$
			$b_w$	$d_w$	$L'$	$t_f$	$d_f$	$A_{v,w}$	$A_{v,f}$		$V_{ACI}$ (kN)	$V_c$	$V_{s-w}$	$V_{s-f}$	$V_P$	
C0	28.8	240	100	280	0	0	0	0.00	0.00	25.54	25.54	0.00	0.00	25.54	1.00	
G1-0.15-3					45	25	33.76			33.76	1.32					
G1-0.30-3					90	70	41.97			41.97	1.64					
G1-0.40-3					120	100	47.44			47.44	1.86					
G1-0.50-3					150	130	52.91			52.91	2.07					
G1-0.65-3					195	175	61.13			61.13	2.39					
G1-0.80-3					240	220	69.34			69.34	2.71					
G1-0.90-3					270	250	74.81			74.81	2.93					
G1-1-3					300	280	76.63			76.63	1.00					
G1-0.15-5					45	25	41.97			41.97	1.64					
G1-0.30-5					90	70	58.39			58.39	2.29					
G1-0.40-5					120	100	69.34			69.34	2.71					
G1-0.50-5					150	130	80.28			80.28	3.14					
G1-0.65-5					195	175	96.71			96.71	3.79					
G1-0.80-5					240	220	113.13			113.13	4.43					
G1-0.90-5					270	250	124.07			124.07	4.86					
G1-1-5				300	280	127.72	127.72	1.00								
C0-S				280	0	0	0	56.6	0	76.26	25.54	50.71	0.00	76.26	1.00	
G3-0.15-3				235	45	25	33.76	42.56	16.10	92.41	1.21					
G3-0.30-3				190	90	70	41.97	34.41	45.07	121.45	1.59					
G3-0.40-3				160	120	100	47.44	28.98	64.38	140.80	1.85					
G3-0.50-3				130	150	130	52.91	23.55	83.70	160.16	2.10					
G3-0.65-3				85	195	175	61.13	15.40	112.67	189.19	2.48					
G3-0.80-3				40	240	220	69.34	7.24	141.64	218.23	2.86					
G3-0.90-3	10	270	250	74.81	1.81	160.96	237.58	3.12								
G3-1-3	0	300	280	76.63	0.00	180.28	256.91	1.00								
G3-0.15-5	235	45	25	41.97	42.56	24.14	108.67	1.43								
G3-0.30-5	190	90	70	58.39	34.41	67.60	160.40	2.10								
G3-0.40-5	160	120	100	69.34	28.98	96.58	194.89	2.56								
G3-0.50-5	130	150	130	80.28	23.55	125.55	229.38	3.01								
G3-0.65-5	85	195	175	96.71	15.40	169.01	281.11	3.69								
G3-0.80-5	40	240	220	113.13	7.24	212.47	332.84	4.36								
G3-0.90-5	10	270	250	124.07	1.81	241.44	367.33	4.82								
G3-1-5	0	300	280	398.14	127.72	0.00	398.14	1.00								

## 6. Numerical Analysis

### 6.1. Model Validation

Thirty-eight FE models (19 without and 19 with stirrups in the web) that are otherwise exactly similar to the test specimens are analyzed. The objective is to evaluate the relative error in using beams without stirrups in the web to estimate the flange contribution to shear strength. The details of models (specimens) are shown in Figure 12a,b. Details of the numerical model are found in El-Azab [30].

### 6.2. Discussion of Results

Table 5 shows the FE results of all 38 models and includes the difference (error) in flange contribution to shear strength calculated using models without stirrups in the web compared to the standard case of models with stirrups. In addition, Figure 13 presents the estimated error in relative flange contribution. It is seen from Figure 13 that the error in relative flange contribution does not exceed  $\pm 5\%$  for  $t_f/h = 0.3$ , does not exceed  $\pm 7\%$  for  $t_f/h = 0.4$ , and ranges from  $+10\%$  to  $+15\%$  for  $t_f/h = 0.5$ . Thus, using a test specimen without stirrups in a web is justified for thin flanges ( $t_f/h \leq 0.4$ ) as the error is marginal. For thicker flanges ( $t_f/h = 0.5$ ), however, the error is always positive and amounts to  $15\%$ .

Thus, the flange contribution obtained from beams without stirrups in the web may be conservatively estimated by reducing it by a factor of  $(1/1.15 \approx 0.87)$ .

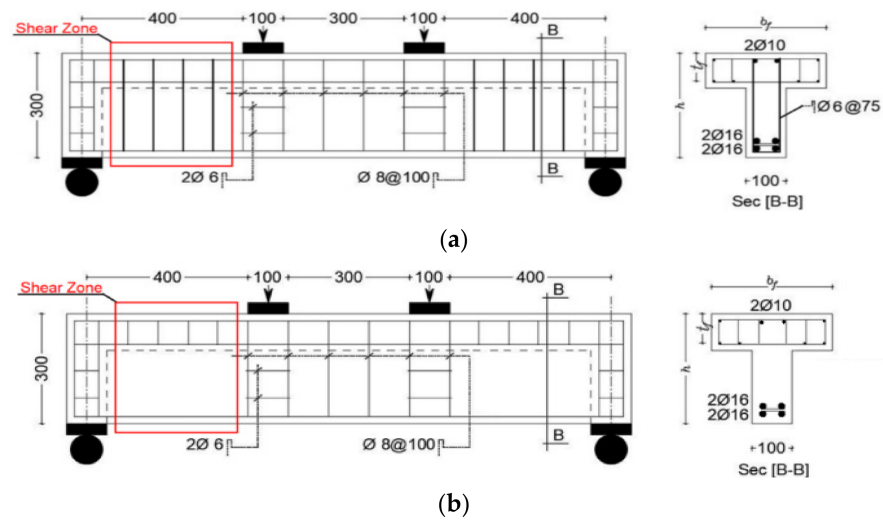


**Figure 12.** Specimen details and arrangement of reinforcement (all dimensions in mm). (a) Specimen with web stirrups within shear zone. (b) Specimen without web stirrups within shear zone.

**Table 5.** The output results for the analyzed specimens.

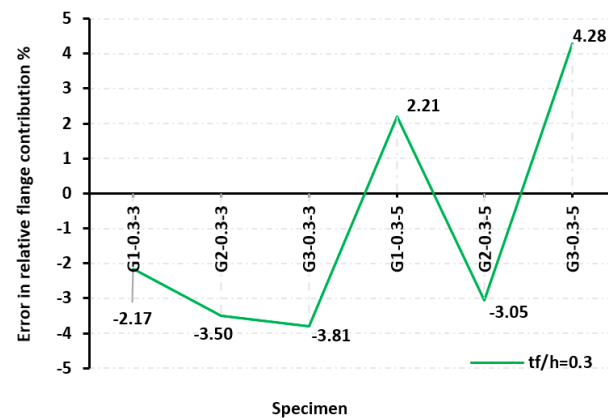
Specimens	$P_u$ (kN) Ansys	Without Stirrups ( $\Delta w$ ) kN	With Stirrups ( $\Delta s$ ) kN	$\frac{\Delta w - \Delta s}{\Delta w} \%$
		$\Delta w =$ $P_{uT} - P_{uC0}$	$\Delta s =$ $P_{uT} - P_{uC0}$	
C0	113.40			
with stir.	232.90			
G1-0.3-3	275.00	161.60		
with stir.	398.00		165.10	−2.17
G2-0.3-3	304.00	190.60		
with stir.	430.16		197.26	−3.50
G3-0.3-3	346.70	233.30		
with stir.	475.08		242.18	−3.81
G1-0.3-5	301.77	188.37		
with stir.	417.11		184.21	2.21
G2-0.3-5	364.38	250.99		
with stir.	491.53		258.64	−3.05
G3-0.3-5	423.32	309.92		
with stir.	529.56		296.66	4.28
G1-0.4-3	358.46	245.06		
with stir.	486.73		253.83	−3.58
G2-0.4-3	368.78	255.38		
with stir.	497.12		264.22	−3.46
G3-0.4-3	375.70	262.30		
with stir.	512.64		279.74	−6.65
G1-0.4-5	401.11	287.71		
with stir.	513.32		280.42	2.53
G2-0.4-5	382.55	269.15		
with stir.	515.13		282.23	−4.86



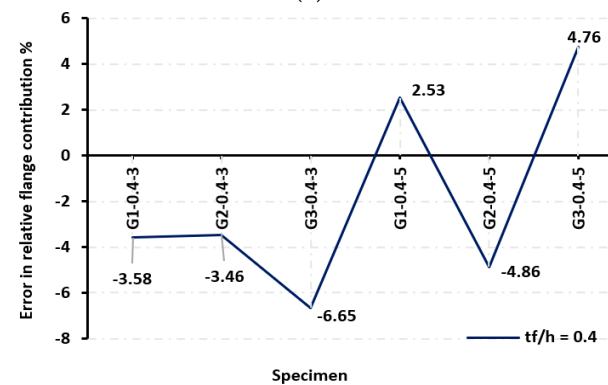
Table 5. Cont.

Specimens	$P_u$ (kN) Ansys	Without Stirrups ( $\Delta w$ ) kN	With Stirrups ( $\Delta s$ ) kN	$\frac{\Delta w - \Delta s}{\Delta w} \%$
		$\Delta w = P_{uT} - P_{uC0}$	$\Delta s = P_{uT} - P_{uC0}$	
G3-0.4-5 with stir.	431.55 535.52	318.15	302.62	4.76
G1-0.5-3 with stir.	434.9 521.54	321.50	288.64	10.22
G2-0.5-3 with stir.	437.392 526.356	323.99	293.46	9.42
G3-0.5-3 with stir.	452.94 540.478	339.54	307.58	9.41
G1-0.5-5 with stir.	420.36 496.87	306.96	263.97	14.01
G2-0.5-5 with stir.	445.85 532.39	332.45	299.49	9.91
G3-0.5-5 with stir.	474.9 542.39	361.50	309.49	14.39

with stir. = Specimen with stirrups in web and flange within shear zone,  $P_{uT}$ : ultimate load of T-section,  $P_{uC0}$ : ultimate load of control specimen.



(a)



(b)

Figure 13. Cont.

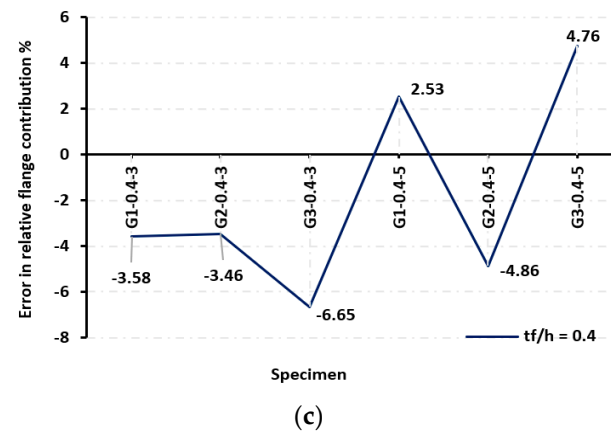


**Figure 13.** Error in relative flange contribution between all tested specimens with and without web stirrups by FE model. They should be listed as: (a) specimens with  $t_f/h = 0.3$ ; (b) specimens with  $t_f/h = 0.4$ ; (c) specimens with  $t_f/h = 0.5$ .

## 7. Conclusions

Based on the presented test and finite element results, and within the limits of the adopted specimens' sizes, arrangement, and reinforcement, the following conclusions were drawn (note that tested beams had no shear reinforcement in the web):

1. The shear capacity of T-beams was notably higher than that of rectangular beams with the same web size. The actual increase depended on the flange dimensions and the amount of reinforcement in the flange. Moreover, the cracking load of T-beams was slightly higher than that of beams without the flange.
2. The flange thickness was the most effective factor in increasing the shear capacity. Increasing the ratio of the flange thickness to total depth ( $\rho_t$ ) from 0.3 to 0.5 increased the shear capacity by 54%, 35%, and 27% for beams without reinforcement, beams with longitudinal reinforcement only, and beams with longitudinal as well as transverse reinforcement, respectively (all refer to flange reinforcement while the web had no shear reinforcement).
3. Increasing the width of the flange had less effect on the shear capacity of T-beams compared to increasing its thickness. For instance, increasing the ratio of the flange width to web width ( $\rho_b$ ) from 3 to 5 increased the shear capacity by 6% to 19%.
4. The use of longitudinal reinforcement in the flange increased its shear strength, and this increase was more pronounced for thinner flanges. In particular, flange reinforcement increased the shear strength by 14% to 43%, 4% to 12%, and 2% to 10% for flange thickness-to-total depth ratios,  $\rho_t$ , of 0.3, 0.4, and 0.5, respectively.
5. The presence of flanges delayed crack propagation, especially for flanges with longitudinal reinforcement.
6. For beams with T-shaped sections with the flange in the compression side, it is conservative to calculate the shear strength of concrete based on the area of the full cross-section. This is true for the assumed limit of  $\rho_b \leq 5$ .
7. The results of this study help in saving construction costs by utilizing the flange's contribution to shear strength for flanged beams with thick flanges in the compression side such as the case of double-cantilevered cap beams with inverted T sections.

**Author Contributions:** Conceptualization, O.M.R. and A.H.A.-K.; methodology, O.M.R., A.H.A.-K., I.A.E.-A. and H.R.A.; software, O.M.R. and I.A.E.-A.; validation, O.M.R., I.A.E.-A. and A.H.A.-K.; formal analysis, O.M.R. and I.A.E.-A.; investigation, O.M.R., A.H.A.-K., I.A.E.-A. and H.R.A.; resources, O.M.R., I.A.E.-A. and A.H.A.-K.; data curation, O.M.R., A.H.A.-K. and H.R.A.; writing—original draft preparation, I.A.E.-A.; writing—review and editing, O.M.R. and A.H.A.-K.; visualization, O.M.R. and A.H.A.-K.; supervision, O.M.R., A.H.A.-K. and H.R.A.; project administration, O.M.R.; funding acquisition, I.A.E.-A. and H.R.A. All authors have read and agreed to the published version of the manuscript.

**Funding:** This research received no external funding.

**Institutional Review Board Statement:** Not applicable.

**Informed Consent Statement:** Not applicable.

**Data Availability Statement:** The data presented in this study are shown in the paper.

**Acknowledgments:** The technical staffs of the Structural Engineering Laboratory of the Faculty deserve special thanks for their assistance in the experimental works of this study.

**Conflicts of Interest:** The authors declare no conflict of interest.

## References

1. Ayensa, A.; Oller, E.; Beltrán, B.; Ibarz, E.; Marí, A.; Gracia, L. Influence of the flange's width and thickness on the shear strength of reinforced concrete beams with T-shaped cross section. *Eng. Struct.* **2019**, *188*, 506–518. [\[CrossRef\]](#)
2. Amna, H.A.; Monstaser, W.M. Shear behavior of reinforced lightweight concrete T-beams. *Life Sci. J.* **2019**, *16*, 11–31.
3. Sarsam, K.; Khalel, R.I.; Mohammed, N. Influence of flange on the shear capacity of reinforced concrete beams. *MATEC Web Conf.* **2018**, *162*, 04003. [\[CrossRef\]](#)
4. Wakjira, T.G.; Ebead, U. Shear span-to-depth ratio effect on steel reinforced grout strengthened reinforced concrete beams. *Eng. Struct.* **2020**, *216*, 110737. [\[CrossRef\]](#)
5. Tetta, Z.C.; Koutas, L.N.; Bournas, D.A. Shear strengthening of concrete members with TRM jackets: Effect of shear span-to-depth ratio, material and amount of external reinforcement. *Compos. Part B Eng.* **2018**, *137*, 184–201. [\[CrossRef\]](#)
6. Hu, B.; Wu, Y.-F. Effect of shear span-to-depth ratio on shear strength components of RC beams. *Eng. Struct.* **2018**, *168*, 770–783. [\[CrossRef\]](#)
7. Samad, A.A.A.; Mohamad, N.; Al-Qershi, M.A.H.; Jayaprakash, J.; Mendis, P. Shear Mechanism and Shear Strength Prediction of Reinforced Concrete T-Beams. *J. Teknol.* **2016**, *78*, 471–476. [\[CrossRef\]](#)
8. Thamrin, R.; Tanjung, J.; Aryanti, R.; Nur, F.; Devinus, A. Shear strength of reinforced concrete T-Beam without stirrups. *J. Eng. Sci. Technol.* **2016**, *11*, 548–562.
9. Mari, A.; Bairan, M.; Cladera, A.; Oller, E.; Rivas, C. Shear flexural strength mechanical model for the design and assessment of reinforced concrete beams Subjected to point or distributed loads. *Front. Struct. Civ. Eng.* **2014**, *8*, 337–353. [\[CrossRef\]](#)
10. Elgohary, A.; Abdelhafiez, A.; Asran, A. Effect of flange width on shear strength of R.C T-beams. *J. Al Azhar* **2019**, *14*, 875–882.
11. Chalioris, C.E.; Zaprís, A.G.; Karayannis, C.G. U-Jacketing Applications of Fiber-Reinforced Polymers in Reinforced Concrete T-Beams against Shear—Tests and Design. *Fibers* **2020**, *8*, 13. [\[CrossRef\]](#)
12. Foster, R.M.; Morley, C.T.; Lees, J.M. Shear Capacity of Reinforced Concrete T-Beams Retrofit with Externally Bonded CFRP Fabric: A New Perspective. *J. Struct. Eng.* **2020**, *146*, 04020253. [\[CrossRef\]](#)
13. Etman, E. External bonded shear reinforcement for T-section beams. *Struct. Concr.* **2011**, *12*, 198–209. [\[CrossRef\]](#)
14. Pohoryles, D.A.; Melo, J.; Rossetto, T. Combined Flexural and Shear Strengthening of RC T-Beams with FRP and TRM: Experimental Study and Parametric Finite Element Analyses. *Buildings* **2021**, *11*, 520. [\[CrossRef\]](#)
15. *ACI Committee Building Code Requirements for Structural Concrete (ACI 318-08) and Commentary (318R-08)*; American Concrete Institute: Farmington Hills, MI, USA, 2008.
16. *CSA Committee A23; Design of Concrete Structure*. Canadian Standards Association: Mississauga, ON, Canada, 2004.
17. European Committee for Standardization. *CEN, EN 1992-1-Eurocode 2: Design of Concrete Structures—Part 1-1: General Rules and Rules for Buildings*; European Committee for Standardization: Brussels, Belgium, 2004.
18. Ioannis, Z.; Maria, K.; Prodromos, Z. Shear Strength of Reinforced Concrete T-Beams. *ACI J.* **2006**, *103*, 693–700.
19. Sahoo, D.R.; Bhagat, S.; Reddy, T.C.V. Experimental study on shear-span to effective-depth ratio of steel fiber reinforced concrete T-beams. *Mater. Struct. Constr.* **2016**, *49*, 3815–3830. [\[CrossRef\]](#)
20. Yehia, B.; Wahab, M. Fracture mechanics of flanged reinforced concrete sections. *Eng. Struct.* **2007**, *29*, 2334–2343. [\[CrossRef\]](#)
21. Pansuk, W.; Sato, Y. Shear Mechanism of Reinforced Concrete T-Beam with Stirrups. *J. Adv. Concr. Technol.* **2007**, *5*, 395–408. [\[CrossRef\]](#)
22. Deifalla, A.; Ghobarah, A. Behavior and analysis of inverted T-shaped RC beams under shear and torsion. *Eng. Struct.* **2014**, *68*, 57–70. [\[CrossRef\]](#)

23. Cladera, A.; Mari, A.; Ribas, C.; Bairán, J.; Oller, E. Predicting the shear–flexural strength of slender reinforced concrete T and I shaped beams. *Eng. Struct.* **2015**, *101*, 386–398. [\[CrossRef\]](#)
24. Ribas Gonzalez, C.R.; Fernández Ruiz, M. Influence of flanges on the shear-carrying capacity of reinforced concrete beams without web reinforcement. *Struct. Concr.* **2017**, *18*, 720–732. [\[CrossRef\]](#)
25. Eswaramoorthi, P.; Prabhu, S.; Palanisamy, M. Experimental Study of Reinforced Concrete Continuous Rectangular and Flanged Beams at Support Region. *Int. J. Civ. Eng. Technol.* **2017**, *8*, 706–713.
26. Huber, P.; Huber, T.; Kollegger, J. Experimental and theoretical study on the shear behavior of single-and multi-span T-and I-shaped post-tensioned beams. *Struct. Concr.* **2020**, *21*, 393–408. [\[CrossRef\]](#)
27. Cavagnis, F.; Ruiz, M.F.; Muttoni, A. An analysis of the shear-transfer actions in reinforced concrete members without transverse reinforcement based on refined experimental measurements. *Struct. Concr.* **2017**, *19*, 49–64. [\[CrossRef\]](#)
28. Premalatha, J.; Shanthi Vengadeshwari, R.; Srihari, P. Finite element modeling and analysis of RC beams with GFRP and steel bars. *Int. J. Civ. Eng. Technol.* **2017**, *8*, 671–679.
29. Montava, I.; Irlés, R.; Segura, J.; Gadea, J.M.; Juliá, E. Numerical Simulation of Steel Reinforced Concrete (SRC) Joints. *Metals* **2019**, *9*, 131. [\[CrossRef\]](#)
30. El-Azab, I.A. Behavior of Flanged Reinforced Concrete Beams Subjected to Shear Force. Ph.D. Thesis, Benha University, Benha, Egypt, 2022; “to appear”. p. 115.